

# On the spheroidization of rod-shaped particles of finite length

F. A. NICHOLS

*Materials and Structural Mechanics, Bettis Atomic Power Laboratory, Westinghouse Electric Corporation, West Mifflin, Pennsylvania, USA*

The governing equation for the capillarity-induced shape changes of a surface of revolution by surface diffusion,

$$\frac{\partial n}{\partial t} = \frac{B}{\gamma} \frac{\partial}{\partial s} \left( \gamma \frac{\partial K}{\partial s} \right)$$

where  $\partial n/\partial t$  is the normal velocity of the surface,  $\gamma$  is measured normal to the axis of revolution,  $s$  is arc length,  $K$  is the total surface curvature and  $B$  is a kinetic parameter which is constant for a given temperature and material, is presented. A numerical solution to this equation is used to analyse finite cylinders with hemispherical ends. A critical length-to-diameter ratio ( $L/D$ ) of 7.2 is predicted, below which only one spheroidal particle results and above which two or more are formed, and is shown to have experimental support in several systems.

## 1. Introduction

The instability of a cylindrical shape under the influence of capillarity or surface tension effects is well-known. First-order perturbation analyses were given by Rayleigh [1] for inviscid fluids both where the fluid flow is within the cylinder (as with a liquid jet) and where the flow is outside the cylinder (as with a gas jet within a liquid). These treatments assumed cylinders of infinite length, thus ignoring end-effects. Analogous treatments were performed by Nichols and Mullins [2] for the kinetic processes of surface (interfacial) diffusion and volume diffusion (both internal and external to the cylinder). The principal results of these analyses are reducible to two characteristic wavelengths, namely  $\lambda_0 = 2\pi R_0$  (where  $R_0$  = initial unperturbed cylindrical radius) and  $\lambda_M$  (a function of the mass-transport mechanism). For any longitudinal perturbation of wavelength less than  $\lambda_0$ , the cylinder is stable, i.e. such perturbations decay with time. For  $\lambda > \lambda_0$ , the cylinder is unstable, i.e. such perturbations increase in amplitude with time. For a wavelength  $\lambda_M$ , the rate at which the perturbation develops

reaches a maximum value. Thus for an actual case in which long cylinders break up due to the chance development of fluctuations in cross-section, one would expect the spacing between the resulting spheroidal particles to coincide closely with  $\lambda_M$ . Nichols and Mullins [2] derived the values  $\lambda_M = 2\pi\sqrt{2}R_0 (= 8.89R_0)$ ,  $9.02R_0$  and  $12.96R_0$  for surface (interfacial) diffusion, internal volume diffusion and external volume diffusion, respectively, as the dominant transport mechanism. These authors also treated the case of an arbitrary ratio of simultaneous surface and external volume diffusivities.

In addition to predicting that long rod-shaped particles (such as precipitates) would spheroidize in the manner described above, Nichols and Mullins further predicted that plate-like particles (or precipitates), being stable with respect to analogous rumpling, would first develop essentially cylindrical (or toroidal) shapes by a bulging process along their edges and these cylindrical shapes would, in turn, spheroidize by the process discussed above.

In another publication [3], Nichols and Mullins

treated the spheroidization of semi-infinite rods by the mechanism of surface (interfacial) diffusion and by numerical techniques analysed the actual shape changes during the entire spheroidization process. Since the bulging of the end of the rod produces a prominent perturbation and allows simultaneous shortening of the rod, one expects intuitively that the sphere-spacing from this "ovulation" process should be somewhat less than that for the infinite cylinder. Indeed, the spacing predicted for the semi-infinite rod for surface diffusion is about  $8.5R_0$  compared with the value of about  $8.9R_0$  for the infinite rod. Although not treated by Nichols and Mullins, the case of a semi-infinite rod ovulating by internal volume diffusion would be expected to produce a very similar spacing since the infinite rod perturbation analysis predicts almost the same spacing as for surface diffusion. By the same token, external volume diffusion should produce significantly greater spacings by a factor of about  $13/9$ , or  $\sim 1.5$ . These various predictions offer numerous possibilities for experimental confirmation and implementation to determine appropriate diffusivities. We shall discuss a number of these applications later.

## 2. Analysis

The significant length of a semi-infinite rod consumed per ovulation event obviously implies what is intuitively apparent a critical length of rod must exist above which ovulation occurs and below which it does not. This presents another parameter which is capable of experimental observation but until now no theoretical predictions have been available. Our purpose here is to supply such predictions for the specific case of surface diffusion.

The surface flux,  $J_s$ , of atoms along an arbitrary surface is [4]

$$J_s = -\frac{D_s \nu}{kT} \nabla_s \mu \quad (1)$$

where  $D_s$  is the surface self-diffusion coefficient (assumed isotropic here),  $\nu$  is the number of diffusing species per unit surface area,  $\mu$  is the chemical potential of the diffusing species,  $k$  and  $T$  have their usual meanings and the gradient in chemical potential,  $\nabla_s \mu$ , is along the surface of interest. Combining Equation 1 with the Gibbs-Thomson relation [4]

$$\mu - \mu_0 = \gamma \Omega K \quad (2)$$

where  $\mu_0$  is the chemical potential of a flat surface  $\gamma$  is the surface tension (assumed isotropic here),  $\Omega$  is the molecular volume and  $K$  is the total curvature of the surface at the point of interest, we have for the special case of a surface of revolution the equation derived previously [3]

$$\frac{\partial n}{\partial t} = \frac{B}{y} \frac{\partial}{\partial s} \left( y \frac{\partial K}{\partial s} \right) \quad (3)$$

where  $\partial n/\partial t$  is the normal velocity of the surface at the point of interest,  $y$  is measured normal to the axis of revolution,  $s$  is arc length along the generating curve for the surface and  $B \equiv D_s \gamma \Omega^2 \nu/kT$  is a constant for a given system at fixed temperature.

A numerical scheme for solving Equation 3 has been presented previously [3] and details will not be repeated here (see also [5]). The solution employs dimensionless variables and the parameter employed here to study the effect of finite rod lengths is the aspect ratio,  $L/D$  or the total tip-to-tip rod length divided by its diameter. That is to say, the starting shapes are perfect finite rods of radius  $R_0$  (diameter  $D$ ) with hemispherical tips also of radius  $R_0$ .  $L/D$  values from 4.75 to 35 were studied. It should be clear that the results obtained apply exactly only to the special shape assumed. Applications to real situations must be made with this fact in mind.

The shape evolution for a rod with an initial  $L/D = 4.75$  is displayed in Fig. 1. The two ends bulge and recede (toward each other). Simultaneously, a slight depression develops at the centre of the rod but it soon reverses itself, an ellipsoidal shape ensues and the final equilibrium spherical shape is approached at long times. These shape changes can be understood in terms of the

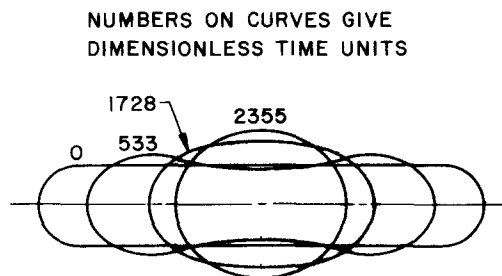


Figure 1 Shape changes for rod of initial aspect ratio of 4.75.

characteristic wavelengths discussed above. For an  $L/D$  of 4.75, there is sufficient length available ( $L = 9.5 R_0$ ) for a wavelength greater than  $\lambda_0 = 6.28 R_0$ ) to develop and so both bulging near the ends and necking in the middle occur. But, as this occurs, the two ends recede (and the two bulges with them), leaving less available length. After  $\tau = 533$  dimensionless time units ( $\tau \equiv (18/\pi r_0)^4 Bt$ , where  $r_0$  = initial rod radius and  $t$  = real time), the length between the maxima in the bulges is only about  $5 R_0 < \lambda_0$ . Thus, at about this point the end effects due to the finite rod length make it impossible for a  $\lambda > \lambda_0$  to exist. Thus, the rod is now stable, the neck expands and eventually a single sphere obtains. This stabilization process is enhanced even more by the fact that the average radius (which is what corresponds to  $R_0$  for the infinite rod) is itself increasing somewhat.

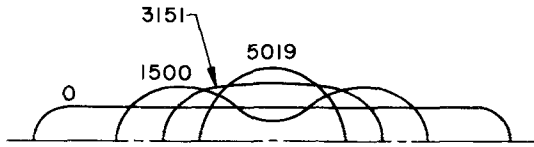


Figure 2 Shape changes for rod of initial aspect ratio of 7.00.

The case of  $L/D = 7.00$  is displayed in Fig. 2 where only half of the symmetrical body is shown. With this longer length ( $L = 14 R_0$ ) an unstable wavelength is maintained longer than before but at  $\tau = 1500$ , the length between bulges is only about  $5.6 R_0 (< \lambda_0)$  and so the neck which in this case has become quite pronounced begins to expand and again a single sphere is the end result.

Critical behaviour is reached at  $L/D = 7.19$  as seen in Fig. 3. The longer length allows the waist to develop until ovulation results, producing two egg-shaped particles at  $\tau = 1461$ . At this critical point the length between bulges is about  $6.3 R_0$ , i.e.

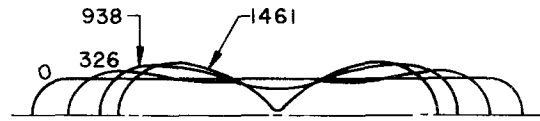


Figure 3 Shape changes for rod of initial aspect ratio of 7.19 (critical aspect ratio).

approximately equal to the critical wavelength for instability of an infinite sphere. In fact, these numbers are surprisingly close ( $\lambda_0 = 6.28 R_0$ ) in that the rod profile at this point differs greatly from a sinusoidal shape.

Since for the critical  $L/D$  the length between bulges at the point of ovulation is just barely sufficient for instability, a somewhat longer rod should result in a longer length at this point and hence yield a faster rate of break-up. That this is in fact the case is shown in Fig. 4, for the case of  $L/D = 7.41$ . The ovulation time has now decreased from  $\tau = 1461$  (for  $L/D = 7.19$ ) to  $\tau = 1415$  (for  $L/D = 7.41$ ). The length between bulges at the time of ovulation for  $L/D = 7.41$  is about 6.8. Since this is still significantly less than  $\lambda_M (= 8.89 R_0$  for surface diffusion) one might expect that a still longer rod should break up faster by developing a longer perturbation. However, such is not the case.

Fig. 5 shows the case of  $L/D = 7.64$  for which a new stabilizing effect begins to be important, i.e. the initial development of a third bulge in the middle. The initial length of  $L = 15.28 R_0$ , being well over  $2\lambda_0 = 12.56 R_0$ , enables the extra bulge to grow until recession of the ends shorten the rod sufficiently to reverse the trend. The net effect of the formation and subsequent elimination of the central bulge is to require a longer time to reach ovulation into two particles at  $\tau = 1435$ .

Longer lengths allow even greater development of the central bulge and thus require still longer times for ovulation. Then, a second critical aspect ratio is reached for the formation of three particles

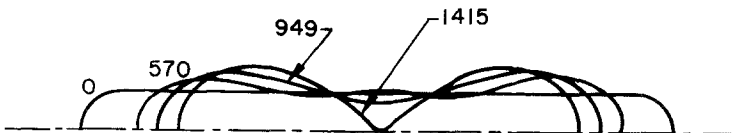
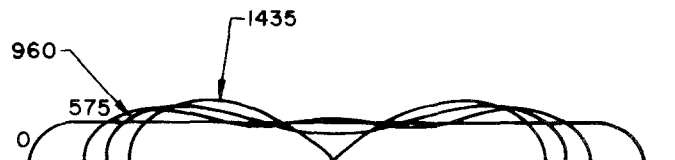


Figure 4 Shape changes for rod of initial aspect ratio of 7.41.

Figure 5 Shape changes for rod of initial aspect ratio of 7.64.



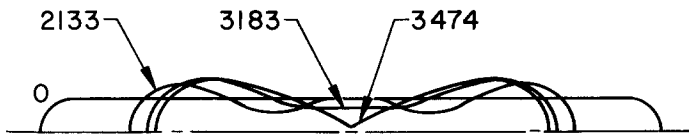


Figure 6 Shape changes for rod of initial aspect ratio of 10.6.

rather than two. Fig. 6 shows the case of an  $L/D$  of 10.6 where separation into three particles is almost possible but eventually the central hump disappears. Ovulation to form two particles then ensues but the time required is now  $\tau = 3474$ , more than a factor of two longer than the minimum ovulation time of  $\tau = 1415$  for an  $L/D$  of 7.41. At an  $L/D$  of about 10.8, three particles are in fact produced with the central one being somewhat smaller. As  $L/D$  increases still further, the ovulation time at first falls as the production of three particles becomes the "natural" process and then increases again as first a fourth bulge forms and then the two central bulges transform into one central bulge. Similar behaviour is expected around critical aspect ratios for forming 4, 5, 6, . . . , etc. particles but the process was not followed in detail beyond the formation of three particles. The longest aspect ratio studied was  $L/D = 35$  and for this case, of course, multiple particles result with the initial ovulation time

being  $\tau = 2471$ . This differs by only  $\sim 7\%$  from the ovulation time obtained previously for a semi-infinite rod which, expressed in these same dimensionless units, would be  $\tau = 2688$ . The variation of ovulation time versus aspect ratio is displayed in Fig. 7. The amplitude of the oscillations in ovulation time of course decreases as the number of particles increases. An error analysis of the numerical scheme employed was presented previously [3, 5]. Based on that analysis, the errors here should be about 1%. Thus, the ovulation time for the semi-infinite rod is better estimated by the  $L/D = 35$  case presented here ( $\tau = 2471$ ) than the value obtained previously with somewhat less accuracy.

The critical aspect ratio obtained here (7.2) below which a finite rod is stable, although precisely correct only for surface diffusion, is expected to be quite accurate for the case of internal volume diffusion since  $\lambda_M$  for internal volume diffusion is only slightly larger than  $\lambda_M$  for surface

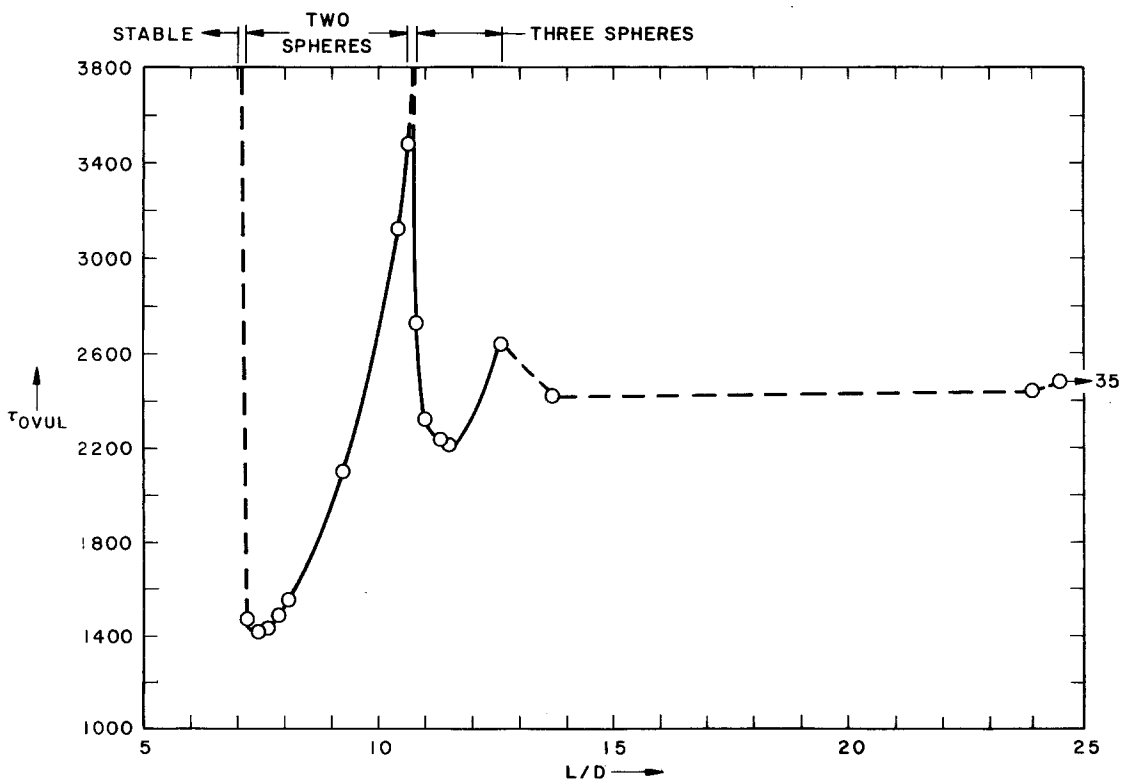


Figure 7 Ovulation time versus aspect ratio.

diffusion. In fact, a very similar critical value should obtain for external volume diffusion as well since  $\lambda_0$  is independent of mechanism and as discussed above, the distance between bulges for the critical aspect ratio at the point of ovulation is essentially equal to  $\lambda_0$ . However, our conclusion for external volume diffusion is clearly not as well founded as for internal volume diffusion.

### 3. Applications to experiment

Moon and Koo [6] studied the development of pores in doped tungsten for use in electric light-bulb filaments. The dopant forms, during processing, gas-filled cavities. Wire drawing stretches these out into long cylinders. During annealing of these long cylindrical pores, ovulation was observed and it was found that the spacing between the resulting spheroidal cavities was in agreement with the  $\lambda_M$  value for surface diffusion predicted by Nichols and Mullins [2]. These authors concluded that surface diffusion was the rate-controlling process and calculated surface diffusivities from the ovulation times which were found to be in satisfactory agreement with values obtained independently by other investigators using other techniques. They further reported that short cylinders ( $L/D \lesssim 10$ ) did not ovulate but instead formed only one spheroidal cavity. Thus, this study confirms the existence of a critical  $L/D$ -ratio but unfortunately its value is only crudely estimated.

Lemlein [7] studied the annealing of saturated salt solution-filled, cylindrical cavities in  $\text{Na}_2\text{NO}_3$  crystals at room temperature. The transparency of the crystals and the relatively large sizes of the cavities (typically  $\geq 6\mu\text{m}$  in diameter) permitted rather detailed, *in situ* observations on their shape evolutions. Many instances of ovulation were observed. The author attributed the rates to the diffusion of salt through the solution inside the cavities, i.e. internal volume diffusion, and for the size of his cavities this seems plausible [2]. Lemlein observed a critical  $L/D$  ratio, below which ovulation did not occur, which from his photographs we estimate to be about 7, in excellent agreement with our predicted value as discussed above. He also observed the behaviour of cylinders not quite sufficiently long to break up. He reports "cases are observed when the nearly elongated inclusion, it would seem, by now ready to be divided into two inclusions, begins to change its shape in a reverse direction, the channel gradually expands and contracts and the two elon-

gated cells connected with it merge into one isometric one". Clearly, he was observing the nearly-critical behaviour we have described above and which is displayed in Fig. 2.

McLean and co-workers [8,9] studied the behaviour of liquid-lead inclusions in aluminium at 450 to 620°C. McLean employed the rigorous Herring scaling laws [10] to show conclusively that the spheroidization of his  $\sim 10\mu\text{m}$  diameter cylinders was controlled by volume diffusion. He presumed, quite plausibly, that Al diffusion within the liquid lead inclusions was rate-controlling. In the absence of a rigorous solution for the detailed volume-diffusion-controlled shape evolutions, he nevertheless was able to predict quantitative rates by ratioing to our solution for surface diffusion in a manner consistent with the Herring scaling laws. McLean also observed that the shorter rods did not ovulate and reported an approximate critical ratio of  $L/D \sim 8$ . Considering that this was given only as a very approximate estimate, we consider it quite consistent with our theoretical prediction of  $\sim 7.2$ .

Stapley and Beevers [11,12] studied the Ostwald ripening of sapphire whiskers embedded in a nickel matrix. For their very small diameters ( $\sim 0.1$  to  $1.4\mu\text{m}$ ) we would definitely expect surface (interfacial) diffusion to control the observed shape changes (assuming the rates are in fact diffusion-controlled), although they did not prove this point. They observed both ovulation from the ends and what they call "waisting" developing from the formation of longitudinal perturbations. They also reported that shorter whiskers did not ovulate but formed only one spheroidal particle. They give a very rough estimate of the critical ratio as  $L/D \sim 6$ . We again consider this very reasonable confirmation of our theoretical predictions, especially in view of the admittedly approximate experimental estimates and the fact that exact values for the critical  $L/D$  ratio will vary for starting shapes departing from our assumed perfect cylinder with hemispherical tips. In general, if the starting shape is more "pointed" than this, the  $L/D$  estimates would be too large whereas for "blunter" starting shapes they would be too small for the proper comparison with theory.

An additional point should be kept in mind when comparing theory and experiment. The numerical technique employed here is capable of handling any surface-of-revolution shape but only

the special shape of a perfect cylinder with hemispherical tips is treated here. A semi-infinite rod with a taper was analysed previously [3] where it was found that if a critical taper is exceeded ( $\sim 3^\circ$ ) ovulation will not occur at all and, for any finite taper ( $> 3^\circ$ ), ovulation times increase significantly. Thus, if experimental studies involve tapered rods, these phenomena must be appropriately factored in when comparing with theory.

Finally, we note that the concept of the spheroidization of cylinders has recently been employed to explain the mechanism of crack healing in ceramic crystals at high temperatures. For example, Yen and Coble [13] report for  $\text{Al}_2\text{O}_3$  that cracks, on annealing, broke up first into channels of cylindrical voids and ultimately into rows of spherical pores. They found the break-up of long cylindrical voids to conform to the Nichols–Mullins theory for surface diffusion but did not address the question of critical  $L/D$  ratios. These studies, however, offer direct experimental support for the mechanism of platelet break-up proposed by Nichols and Mullins [2], i.e. platelet  $\rightarrow$  cylinders (on the platelet edges)  $\rightarrow$  spheres (by ovulation from cylinders).

#### 4. Conclusions

The evolution in shape of finite, initially cylindrical rods due to capillarity-induced surface diffusion has been developed by a numerical solution of the controlling differential equation.

A critical length-to-diameter ratio ( $L/D$ ) of 7.2 is predicted, below which a rod will form one spheroid and above which it will form two or more. This predicted critical  $L/D$  value was shown to have experimental support from several studies. Also, experimental evidence was discussed for the validity of the previously proposed mechanism for the break-up of platelets into cylinders and finally into spheres.

#### References

1. LORD RAYLEIGH, *Proc. London Math. Soc.* **10** (1878) 4.
2. F. A. NICHOLS and W. W. MULLINS, *Trans. Met. Soc. AIME* **233** (1965) 1840.
3. F. A. NICHOLS and W. W. MULLINS, *J. Appl. Phys.* **36** (1965) 1826.
4. W. W. MULLINS, *J. Appl. Phys.* **28** (1957) 333.
5. F. A. NICHOLS, *Acta Met.* **16** (1968) 103.
6. D. M. MOON and R. C. KOO, *Met. Trans.* **2** (1971) 2115.
7. G. G. LEMMLEIN, *Proc. USSR Acad. Sci.* **85** (1952) 1.
8. M. McLEAN, *Phil. Mag.* **27** (1973) 1253.
9. M. McLEAN and M. S. LOVEDAY, *J. Mater. Sci.* **9** (1974) 1104.
10. C. HERRING, *J. Appl. Phys.* **21** (1950) 301.
11. A. J. STAPLEY and C. J. BEEVERS, *J. Mater. Sci.* **8** (1973) 1287.
12. *Idem, ibid* **8** (1973) 1296.
13. C. F. YEN and R. L. COBLE, *J. Amer. Ceram. Soc.* **55** (1972) 507.

Received 28 October and accepted 17 November 1975.